Supplementary Material

Synthesis, computational and nanoencapsulation studies on eugenol-derived insecticides

Catarina M. M. Coelho[a], Renato B. Pereira[b], Tatiana F. Vieira[c,d], Cláudia M. Teixeira[a,b], Maria José G. Fernandes[a], Ana Rita O. Rodrigues[e,f], David M. Pereira[b], Sérgio F. Sousa[c,d], A. Gil Fortes[a], Elisabete M. S. Castanheira[e] and M. Sameiro T. Gonçalves[a,*]

[a] *Centre of Chemistry, Department of Chemistry, University of Minho, Campus of Gualtar, 4710-057 Braga, Portugal;*

[b]*REQUIMTE/LAQV, Laboratory of Pharmacognosy, Department of Chemistry, Faculty of Pharmacy, University of Porto, R. Jorge Viterbo Ferreira, 228, 4050-313 Porto, Portugal;*

[c] *UCIBIO/REQUIMTE, BioSIM – Departamento de Medicina, Faculdade de Medicina da Universidade Do Porto, Alameda Prof. Hernâni Monteiro, 4200-319 Porto, Portugal;*

[d] *Associate Laboratory i4HB - Institute for Health and Bioeconomy, Faculdade de Medicina, Universidade do Porto, 4200-319 Porto, Portugal;*

[e] *Physics Centre of Minho and Porto Universities (CF-UM-UP), University of Minho, Campus of Gualtar, 4710-057 Braga, Portugal;*

[f]*Associate Laboratory LaPMET - Laboratory of Physics for Materials and Emergent Technologies, University of Minho, Campus of Gualtar, 4710-057 Braga, Portugal.*

Table S1. Targets selected for the inverted virtual screening assay

Target	Organism	PDB target	Resolution (Å)	Description	Ref
Ecdysone receptor	*Heliothis virescens*	1R20	3.00	VS based on 1R20 bound to an agonist as a model for the development of a receptor-based pharmacophore model.	1
		1R1K	2.90	VS of 2 million compounds against 1R1K, an ecdysone receptor structure bound to its known ligand ponasterone A.	2
Chitinase	*Ostrinia furnacalis*	3WL1	1.77	Pharmacophore-based screening using two crystal structures of chitinases: 3WL1 bound to its reaction product and 3WQV bound to an inhibitor.	3
		3WQV	2.04		
beta-*N*-Acetyl-D-hexosaminidase OfHex1		3NSN	2.10	VS of the ZINC database to identify OfHex1 inhibitors using 3NSN crystal structure bound to a known inhibitor.	4
		3OZP	2.00	VS of the ZINC data-base targeting 3OZP, a crystal structure of OfHex1 bound to an inhibitor.	5
N-Acetylglucosamine-1-phosphate uridyltransferase (GlmU)	*Xanthomonas oryzae*	2V0K	2.30	Homology model built for docking using 2V0K and 2VD4 as templates. 2V0K crystal structure is bound to its known ligand and 2VD4 is bound to a possible inhibitor.	6
		2VD4	1.90		
Acetylcholinesterase	*Aedes aegypti*	1QON	2.72	Search for new molecules with insecticidal activity against *Ae. Aegypti* using acetylcholinesterase crystal structures 1QON and 4EY6 as targets, both bound to possible inhibitors.	7
		4EY6	2.40		
	Drosophila melanogaster	1DX4	2.70	Homology 3D model built for VS using 1DX4 as template. 1DX4 crystal structure is bound to a potent inhibitor.	8
Prophenoloxidase (PPO)	*Manduca sexta*	3HSS	1.97	Crystal structure of a prophenoloxidase from *Manduca sexta*.	9
p-Hydroxyphenyl-pyruvate dioxygenase	*Arabidopsis thaliana*	6ISD	2.40	Development of a receptor-ligand pharmacophore model based on the crystal structure 6ISD bound to a commonly used pesticide. The best model created was then used for VS studies.	10
Voltage-gated sodium channel	*Periplaneta americana*	6A95	2.60	Crystallographic structure of a Voltage-gated sodium channel NavPaS bound to a pore blocker, tetrodotoxin (TTX)	11
Octopamine receptor	*Blattella germanica*	4N7C	1.75	Crystal structure of Bla g 4, an octopamine receptor, bound to tyramine.	12
Sterol carrier protein-2 (HaSCP-2)	*Helicoverpa armigera*	4UEI	Solution NMR	Structure-based VS of a database of commercially available compounds to find potential inhibitors of HaSCP-2. The residues Phe53, Thr128, and Gln131 were selected for the binding cavity.	13
Peptide deformylase	*Xanthomonas oryzae*	5CY8	2.38	Docking and VS of a library of 318 phytochemicals. 5CY8 crystal structure is bound to a possible inhibitor.	14
Alpha-esterase-7 (αE7)	*Lucilia cuprina*	5TYJ	1.75	Computational design of potent and selective covalent inhibitors of αE7. 5TYJ and 5TYP crystal structures are bound to inhibitors: (3-bromo-5-phenoxylphenyl)boronic acid and (3-bromo-4-methylphenyl)boronic acid respectively.	15
		5TYP	1.88		
Odorant Binding Protein	*Aedes aegypti*	5V13	1.84	Search for new molecules with insecticidal activity against *Ae. Aegypti* using a crystal structure of a mosquito juvenile hormone-binding protein, 5V13 bound to its natural hormone.	7
	Drosophila melanogaster	2GTE	1.40	2GTE crystal structure is bound to its natural ligand	16
	Anopheles gambiae	3N7H	1.60	QSAR and docking studies for the rational design of mosquito repellents using the crystal structure 3K1E bound to a polyethylene glycol molecule. 3N7H crystal structure is bound to a commonly used repellent.	17
	Aedes aegypti	3K1E	1.85		17

Creation of a homology model

The model generated by SWISS-MODEL for 1QON was used in the MD simulations since the gap that was missing from the original structure was distant from the active site.

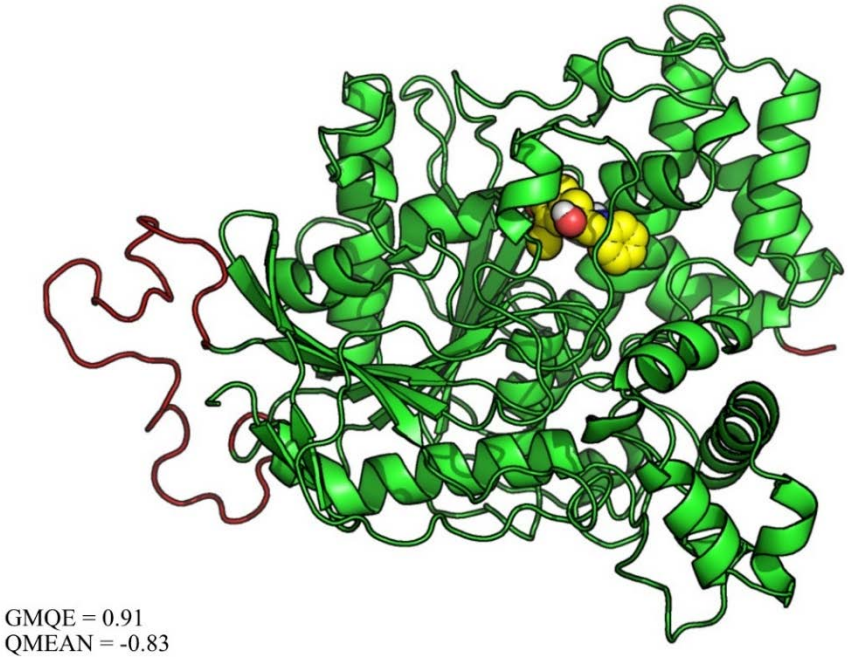

Figure S1. Homology model built for 1QON. Green is the original structure and red represents the loop that was generated by SWISS-MODEL. In yellow is the ligand molecule (NP34). GMQE - Global Model Quality Estimation, is expressed between 0 and 1 with a higher number meaning higher reliability. QMEAN - provides an estimate of the "degree of nativeness" of the structural features observed in the model. A value of QMEAN around zero indicate a good agreement between the model and experimental structure.

Figure S2. Protein and ligand RMSD (Å) of the AChE and OBP – ligand complexes.

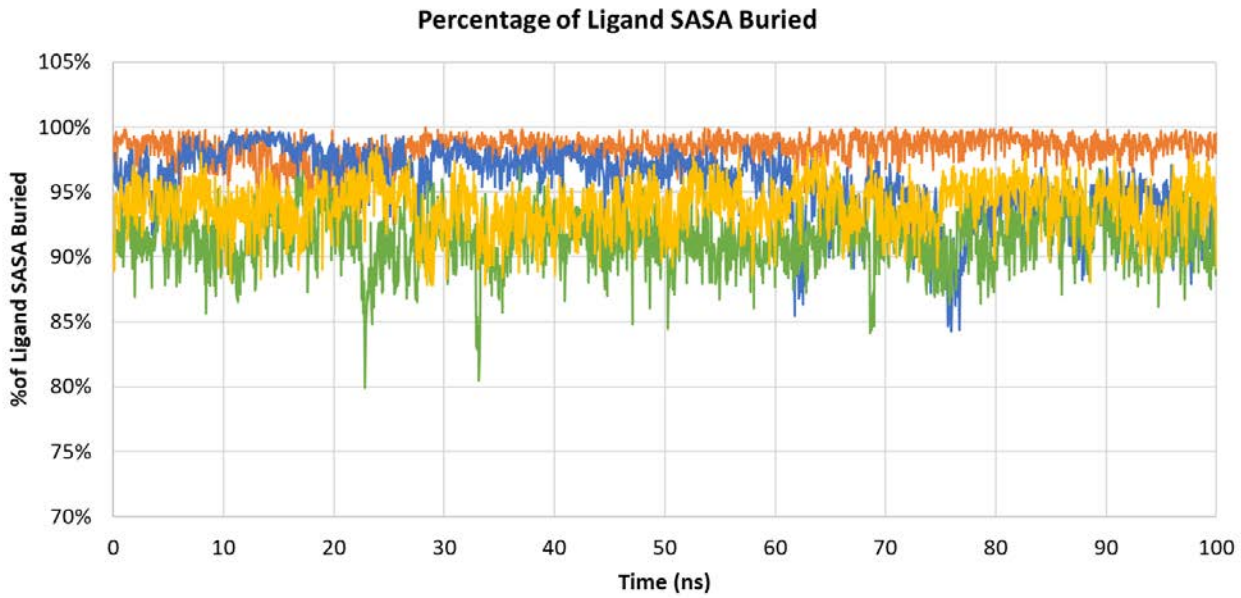

Figure S3. Percentage of the potential solvent accessible surface area of the ligands that is buried by the protein targets evaluated.

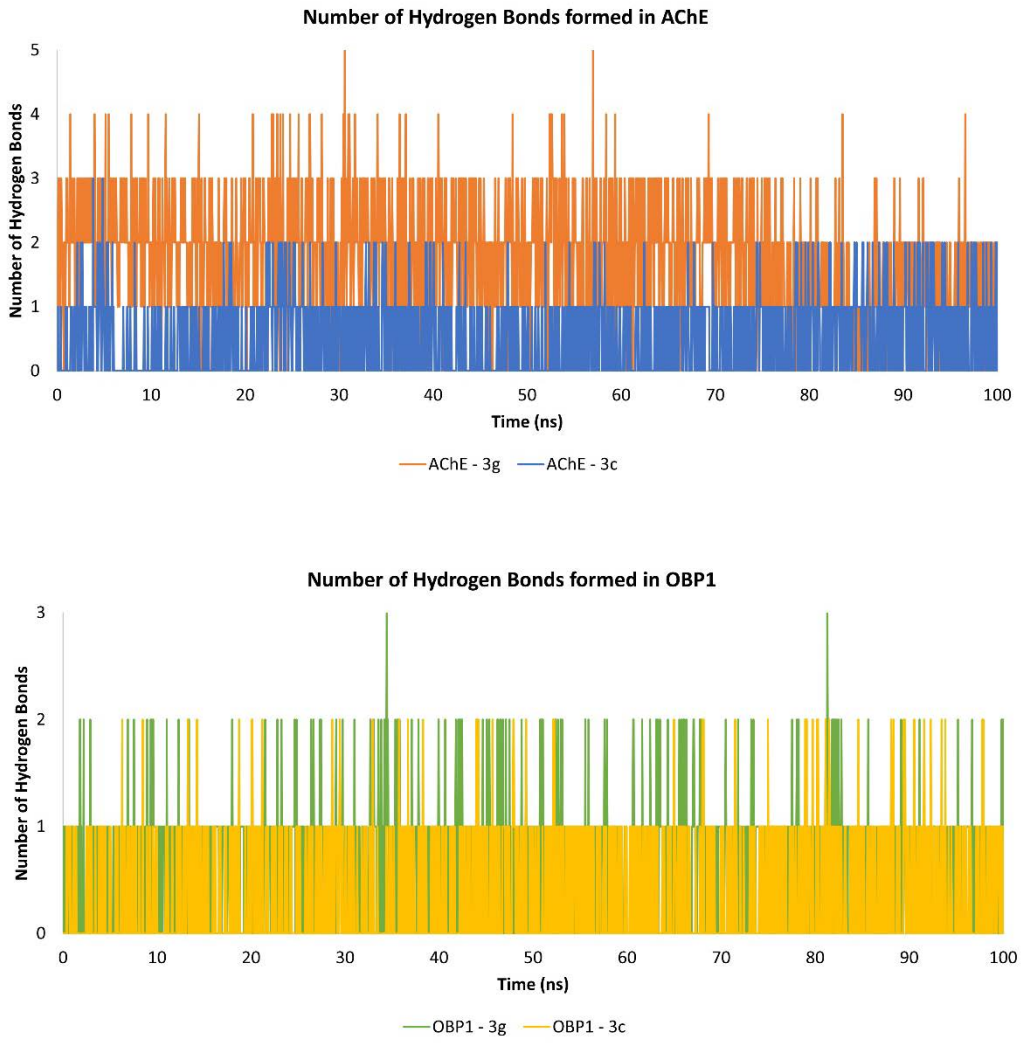

Figure S4. Number of ligand-target hydrogen bonds formed during the simulations for compound **3d** and **3f** when complexed with AchE and OBP.

Table S2. Docking scores for Compound **3c** and **3g** in complex with Human and insect AChE.

		PLP	ASP	ChemScore	GoldScore	Vina
Human AChE	3c	69.19	45.37	35.79	55.49	-7.3
Insect AChE	3c	72.89	51.12	32.77	59.90	-7.5
Human AChE	3g	82.93	54.23	39.29	65.03	-8.5
Insect AChE	3g	96.52	60.47	39.41	69.58	-9.0

References

(1) Hu, X.; Yin, B.; Cappelle, K.; et al. Identification of novel agonists and antagonists of the ecdysone receptor by virtual screening, *J. Mol. Graph Model.* **2018**, 81, 77-85.

(2) Harada, T.; Nakagawa, Y.; Ogura, T.; Yamada, Y.; Ohe, T.; Miyagawa, H. Virtual Screening for Ligands of the Insect Molting Hormone Receptor, *J. Chem. Inf. Model.* **2011**, 51(2), 296-305.

(3) Dong, Y.; Jiang, X.; Liu, T.; et al. Structure-Based Virtual Screening, Compound Synthesis, and Bioassay for the Design of Chitinase Inhibitors, *J. Agric. Food Chem.* **2018**, 66, 3351-3357.

(4) Liu, J.; Liu, M.; Yao, Y.; et al. Identification of Novel Potential β-N-Acetyl-D-Hexosaminidase Inhibitors by Virtual Screening, Molecular Dynamics Simulation and MM-PBSA Calculations. *Int. J. Mol. Sci.* **2012**, 13, 4545-4563.

(5) Dong, L.; Shen, S.; Xu, Y.; et al. Identification of novel insect β-N-acetylhexosaminidase OfHex1 inhibitors based on virtual screening, biological evaluation, and molecular dynamics simulation. *J. Biomol. Struct. Dyn.* **2021**, 39, 1735-1743.

(6) Min, J.; Lin, D.; Zhang, Q.; Zhang, J.; Yu, Z; Structure-based virtual screening of novel inhibitors of the uridyltransferase activity of Xanthomonas oryzae pv. oryzae GlmU. *Eur. J. Med. Chem.* **2012**, 53, 150-158.

(7) Ramos, R.; Costa, J.; Silva, R.; et al. Identification of Potential Inhibitors from Pyriproxyfen with Insecticidal Activity by Virtual Screening. *Pharmaceuticals* **2019**, 12, 20.

(8) Riva, C.; Suzanne, P.; Charpentier, G.; Dulin, F.; Halm-Lemeille, M.-P.; Sopkova-de Oliveira Santos, J. In silico chemical library screening and experimental validation of novel compounds with potential varroacide activities, *Pestic. Biochem. Physiol.* **2019**, 160, 11-19.

(9) Li, Y.; Wang, Y.; Jiang, H.; Deng, J. Crystal structure of Manduca sexta prophenoloxidase provides insights into the mechanism of type 3 copper enzymes, *Proc. Natl. Acad. Sci.* **2009**, 106, 17002-17006.

(10) Fu, Y.; Liu, Y.-X.; Kang, T.; Sun, Y.-N.; Li, J.-Z.; Ye, F. Identification of novel inhibitors of p-hydroxyphenylpyruvate dioxygenase using receptor-based virtual screening, *J. Taiwan Inst. Chem. Eng.* **2019**, 103, 33-43.

(11) Shen, H.; Li, Z.; Jiang, Y.; et al. Structural basis for the modulation of voltage-gated sodium channels by animal toxins, *Science* **2018**, 362(6412), 1-8.

(12) Offermann, L.R.; Chan, S.L.; Osinski, T.; Tan, Y.W.; Chew, F.T.; Sivaraman, J.; Mok, Y.-K.; Minor, W.; Chruszcz, M. The major cockroach allergen Bla g 4 binds tyramine and octopamine, *Mol. Immunol.* **2014**, 60, 86-94.

(13) Cai, J.; Du, X.; Wang, C.; Lin, J.; Du, X. Identification of Potential Helicoverpa armigera (Lepidoptera: Noctuidae) Sterol Carrier Protein-2 Inhibitors Through High-Throughput Virtual Screening, *J. Econ. Entomol.* **2017**, 110, 1779-1784.

(14) Joshi, T.; Joshi, T.; Sharma, P.; Chandra, S.; Pande, V. Molecular docking and molecular dynamics simulation approach to screen natural compounds for inhibition of Xanthomonas oryzae pv. Oryzae by targeting peptide deformylase. *J. Biomol. Struct. Dyn.* **2021**, 39, 823-840.

(15) Correy, G. J.; Zaidman, D.; Harmelin, A.; et al. Overcoming insecticide resistance through computational inhibitor design. *Proc. Natl. Acad. Sci.* **2019**, 116, 21012-21021.

(16) Laughlin, J.D.; Ha, T.S.; Jones, D.N.M.; Smith, D.P. Activation of Pheromone-Sensitive Neurons Is Mediated by Conformational Activation of Pheromone-Binding Protein, *Cell* **2008**, 13, 1255-1265.

(17) Oliferenko, P.V.; Oliferenko, A.A.; Poda, G.I.; et al. Promising Aedes aegypti Repellent Chemotypes Identified through Integrated QSAR, Virtual Screening, Synthesis, and Bioassay. Oliveira, P.L. Editor, *PLoS One*, **2013**, 8, e64547.

*^{1}H and ^{13}C NMR spectra of compounds **3a-g***

^{1}H NMR spectra of compounds **3a-g** are shown. These spectra confirm the corresponding structure and purity of each compound. In addition, ^{13}C spectra are also shown. This information serves as the statement for confirming the purity (≥95%) of the compounds synthesized in the reported work.

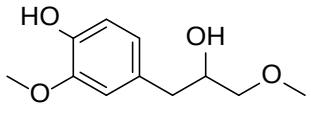

3a

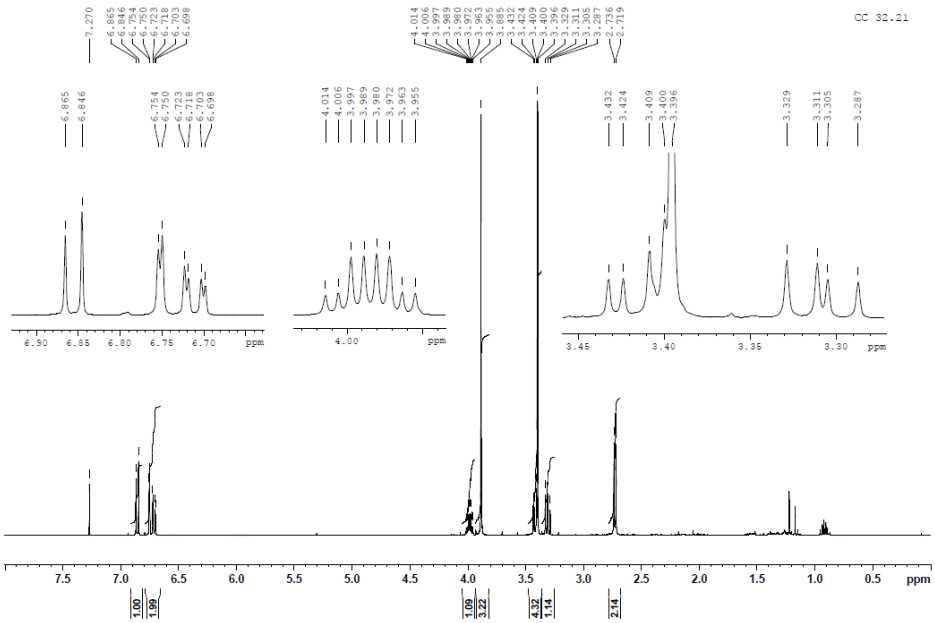

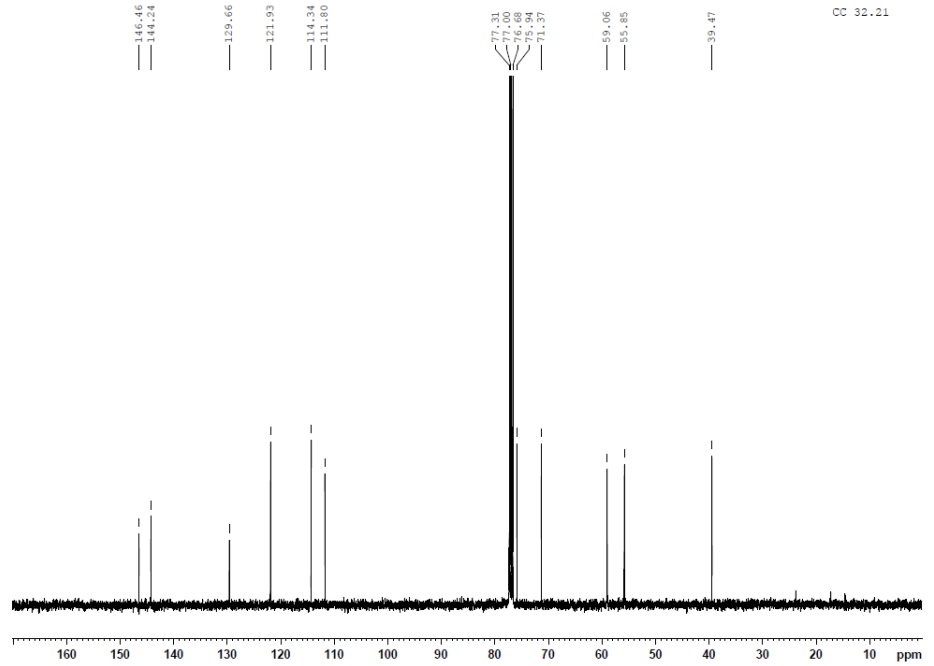

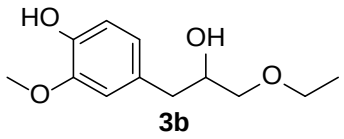
HO
OH
O
O

3b

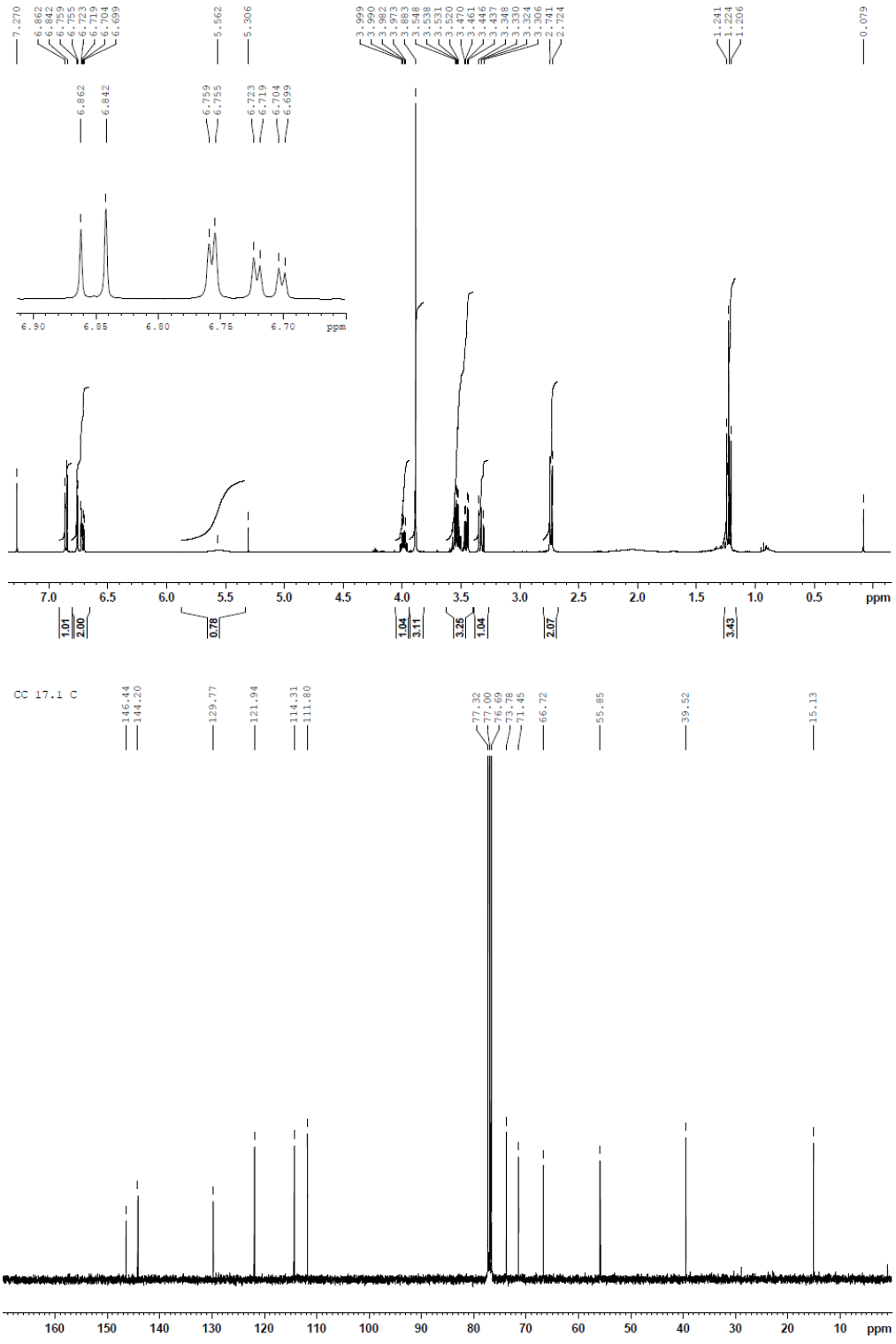
7.270
6.862
6.842
6.759
6.755
6.723
6.719
6.704
6.699
5.562
5.306
3.999
3.990
3.982
3.973
3.883
3.548
3.538
3.531
3.520
3.470
3.461
3.446
3.437
3.348
3.330
3.324
3.306
2.741
2.724
1.241
1.224
1.206
0.079
6.862
6.842
6.759
6.755
6.723
6.719
6.704
6.699
6.90
6.85
6.80
6.75
6.70
ppm
7.0
6.5
6.0
5.5
5.0
4.5
4.0
3.5
3.0
2.5
2.0
1.5
1.0
0.5
ppm
1.07
2.00
0.70
1.04
3.11
3.25
1.04
2.07
3.43
CC 17.1 C
146.44
144.20
129.77
121.94
114.31
111.80
77.32
77.00
76.68
73.78
71.45
66.72
55.85
39.52
15.13
160
150
140
130
120
110
100
90
80
70
60
50
40
30
20
10
ppm

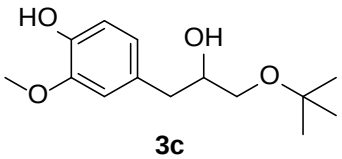
HO
OH
O
O

3c

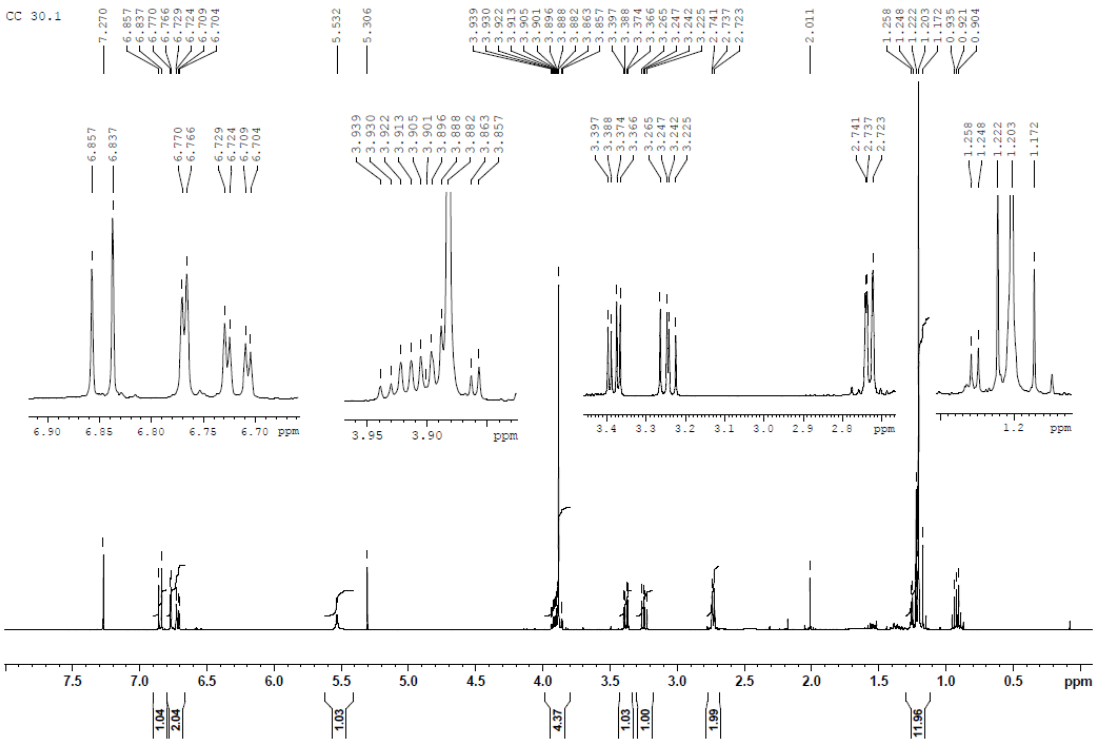
CC 30.1
7.270
6.857
6.837
6.770
6.766
6.729
6.724
6.709
6.704
5.532
5.306
3.939
3.930
3.922
3.913
3.905
3.901
3.896
3.888
3.882
3.863
3.857
3.397
3.388
3.374
3.366
3.265
3.247
3.242
3.225
2.741
2.737
2.723
2.011
1.258
1.248
1.222
1.203
1.172
0.935
0.921
0.904
ppm
1.04
2.04
1.03
4.37
1.03
1.00
1.99
11.96

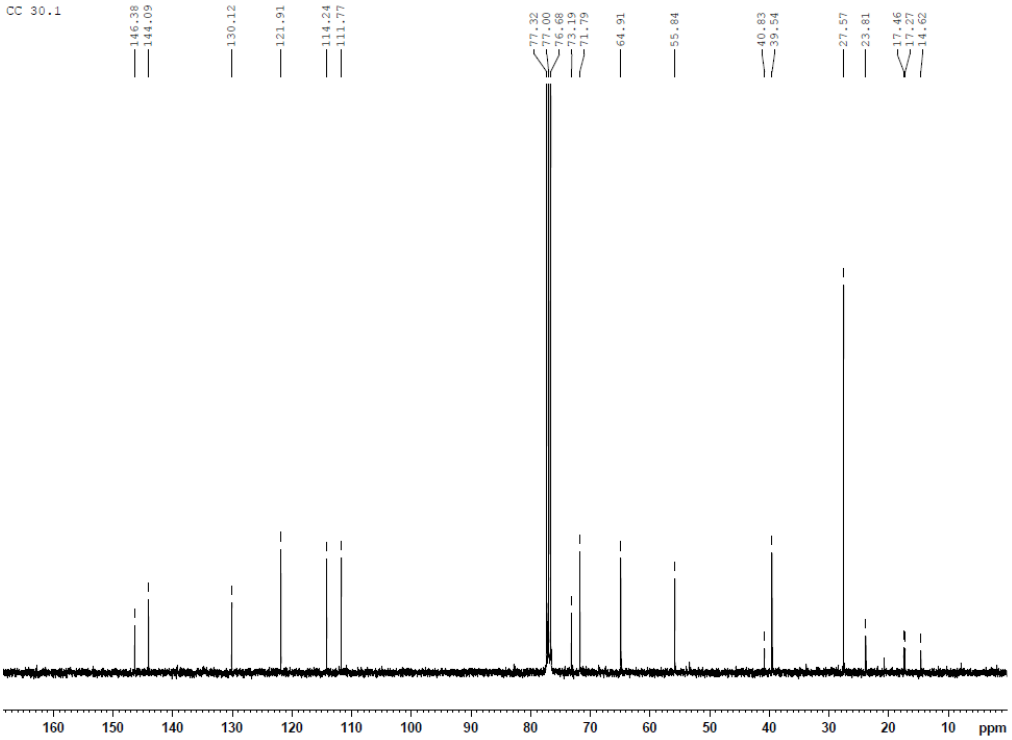
CC 30.1
146.38
144.09
130.12
121.91
114.24
111.77
77.32
77.00
76.68
73.19
71.79
64.91
55.84
40.83
39.54
27.57
23.81
17.46
17.27
14.62
ppm

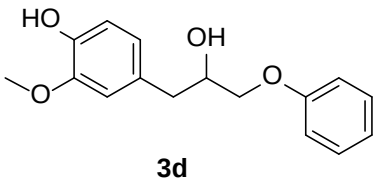
HO
OH
O
O

3d

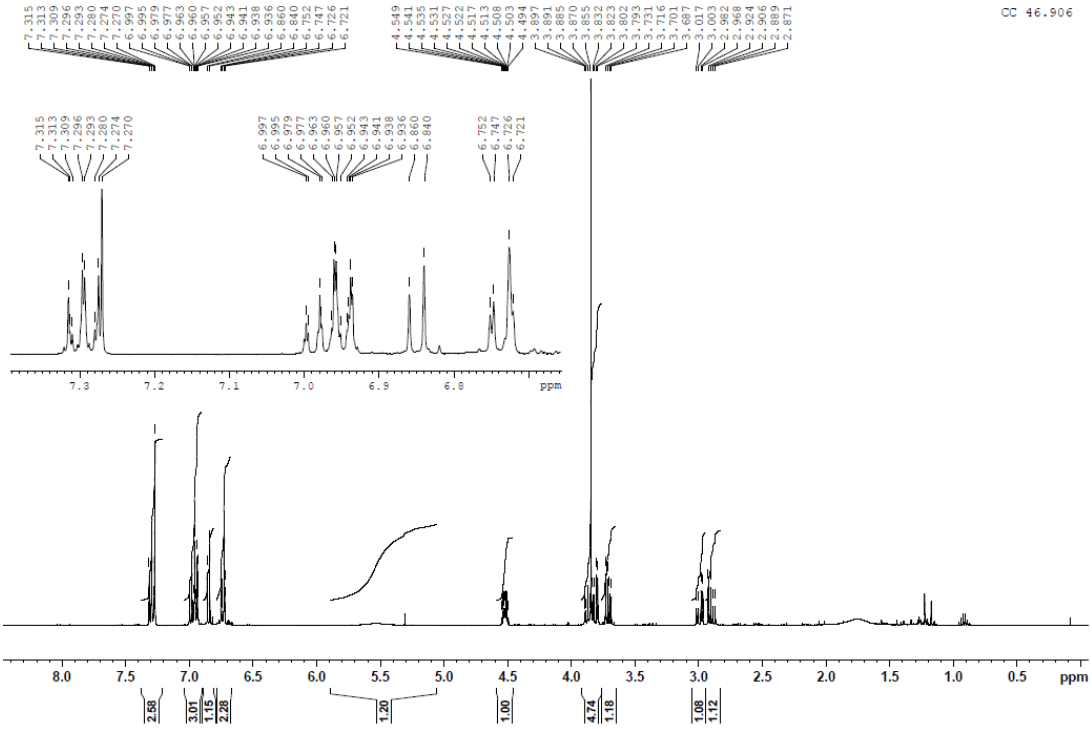
CC 46.906
8.0
7.5
7.0
6.5
6.0
5.5
5.0
4.5
4.0
3.5
3.0
2.5
2.0
1.5
1.0
0.5
ppm
2.58
3.01
1.15
2.28
1.20
1.00
4.74
1.18
1.08
1.12

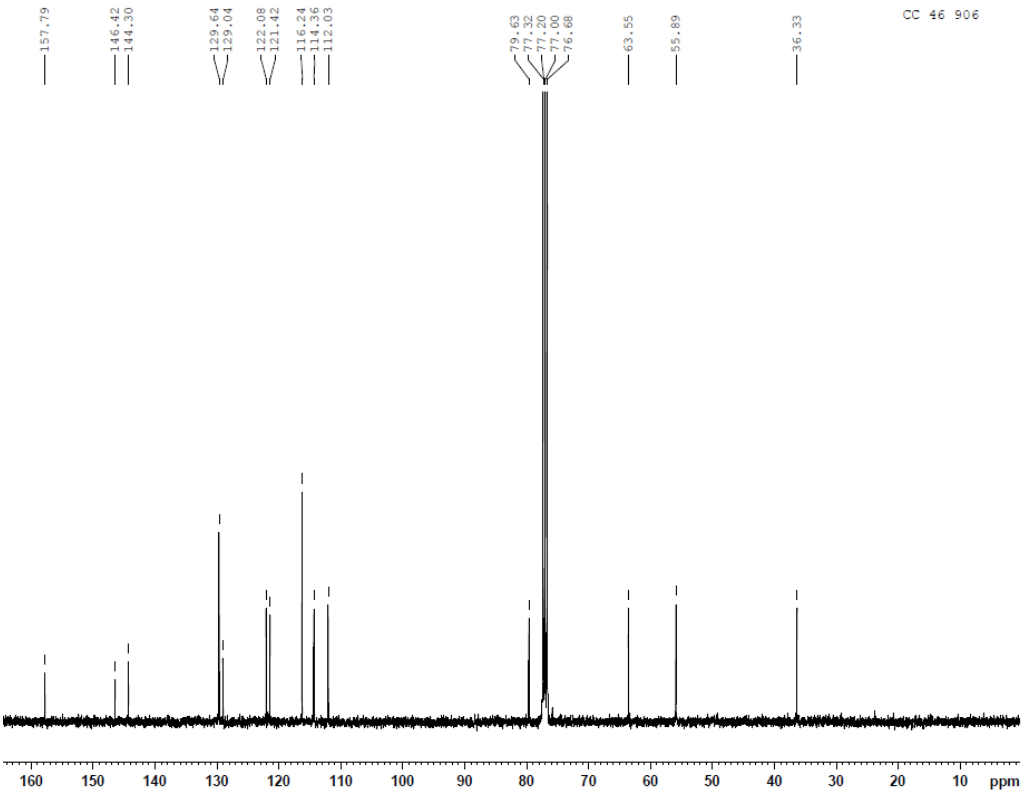
CC 46 906
157.79
146.42
144.30
129.64
129.04
122.08
121.42
116.24
114.36
112.03
79.63
77.32
77.20
77.00
76.68
63.55
55.89
36.33
160
150
140
130
120
110
100
90
80
70
60
50
40
30
20
10
ppm

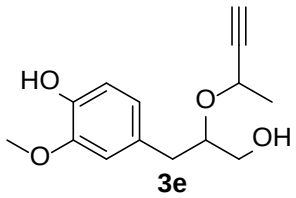
HO
O
OH
O

3e

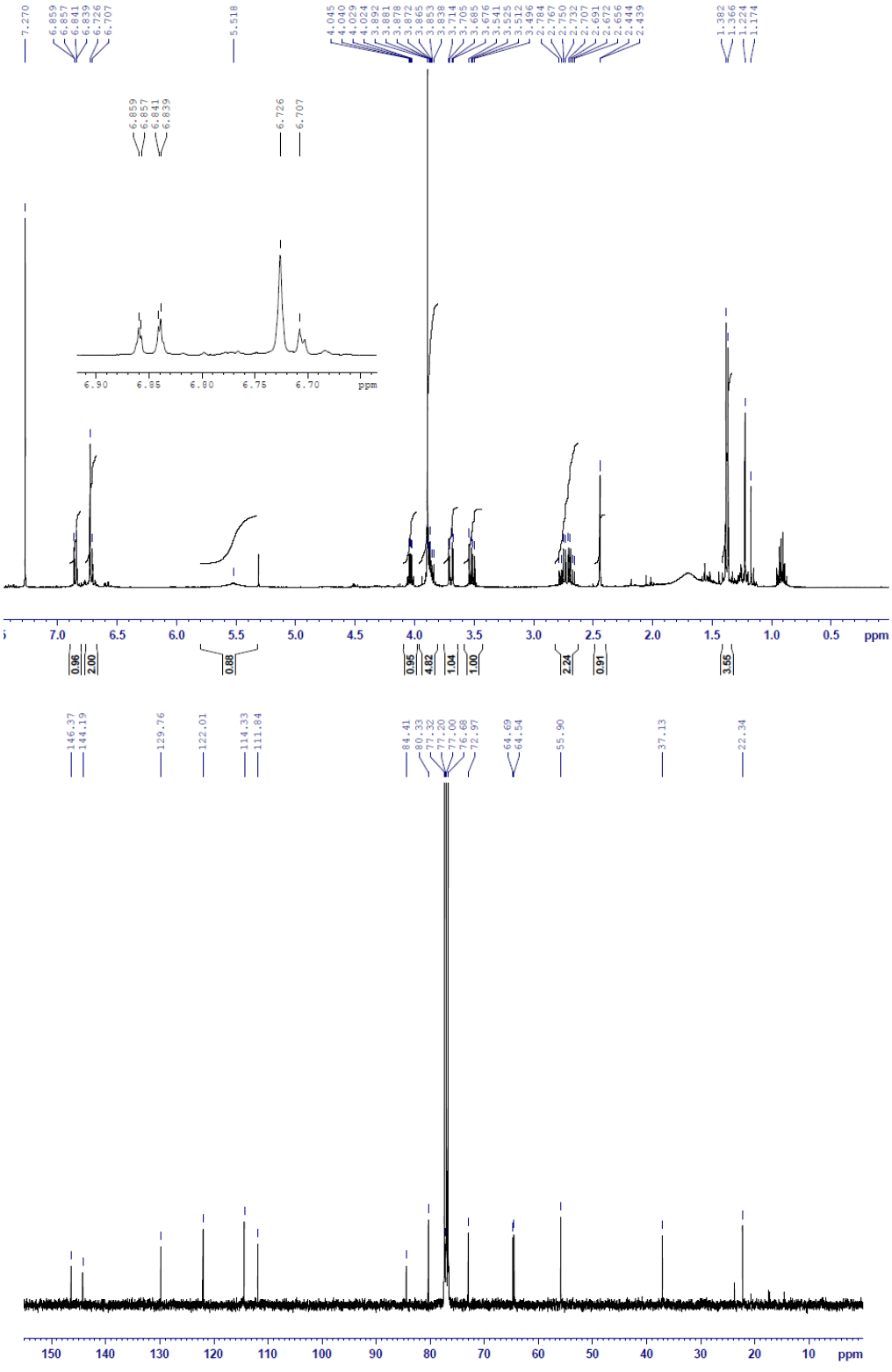
7.270
6.859
6.857
6.841
6.839
6.726
6.707
5.518
4.045
4.040
4.029
4.024
3.892
3.881
3.878
3.872
3.865
3.853
3.838
3.714
3.705
3.685
3.676
3.541
3.525
3.512
3.496
2.764
2.757
2.750
2.732
2.707
2.691
2.672
2.656
2.444
2.439
1.382
1.366
1.224
1.174
ppm
0.96
2.00
0.88
0.95
4.82
1.04
1.00
2.24
0.91
3.66
146.37
144.19
129.76
122.01
114.33
111.84
84.41
80.33
77.32
77.00
76.68
72.97
64.69
64.54
55.90
37.13
22.34

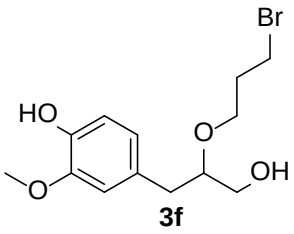
Br
HO
O
OH
O

3f

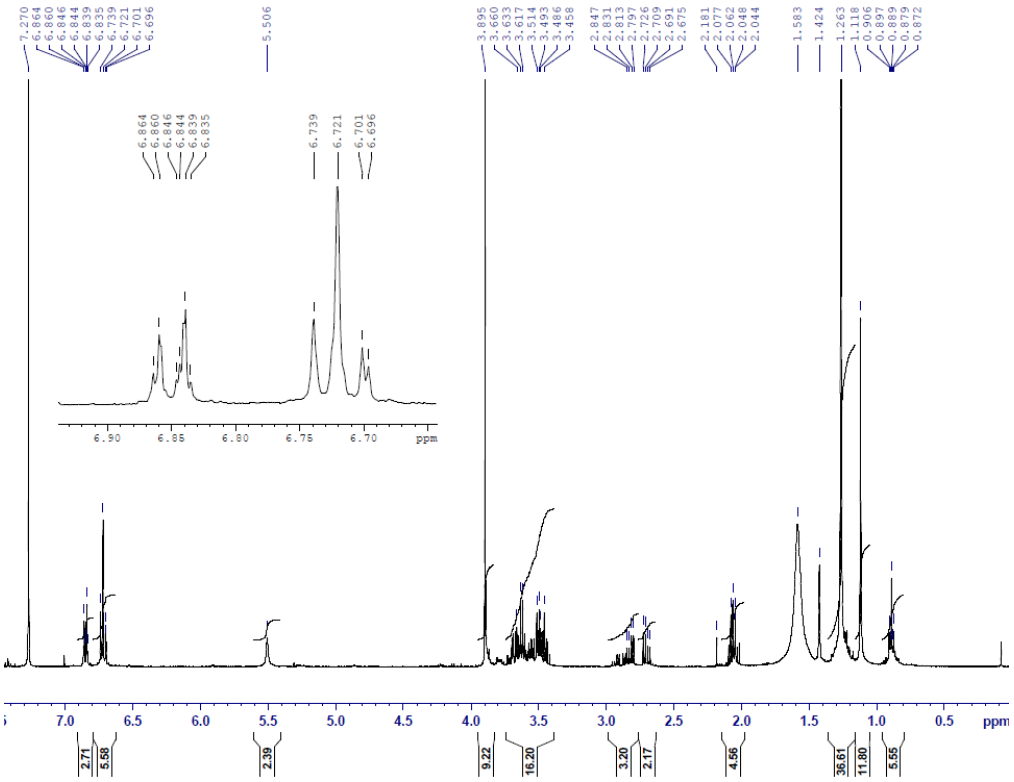
7.270
6.864
6.860
6.846
6.844
6.839
6.835
6.739
6.721
6.701
6.696
5.506
3.895
3.660
3.633
3.617
3.514
3.493
3.486
3.458
2.847
2.831
2.813
2.797
2.726
2.709
2.691
2.675
2.181
2.077
2.062
2.048
2.044
1.583
1.424
1.263
1.118
0.906
0.897
0.889
0.879
0.872
ppm
2.71
5.68
2.39
9.22
16.20
3.20
2.17
4.56
36.61
11.80
5.55

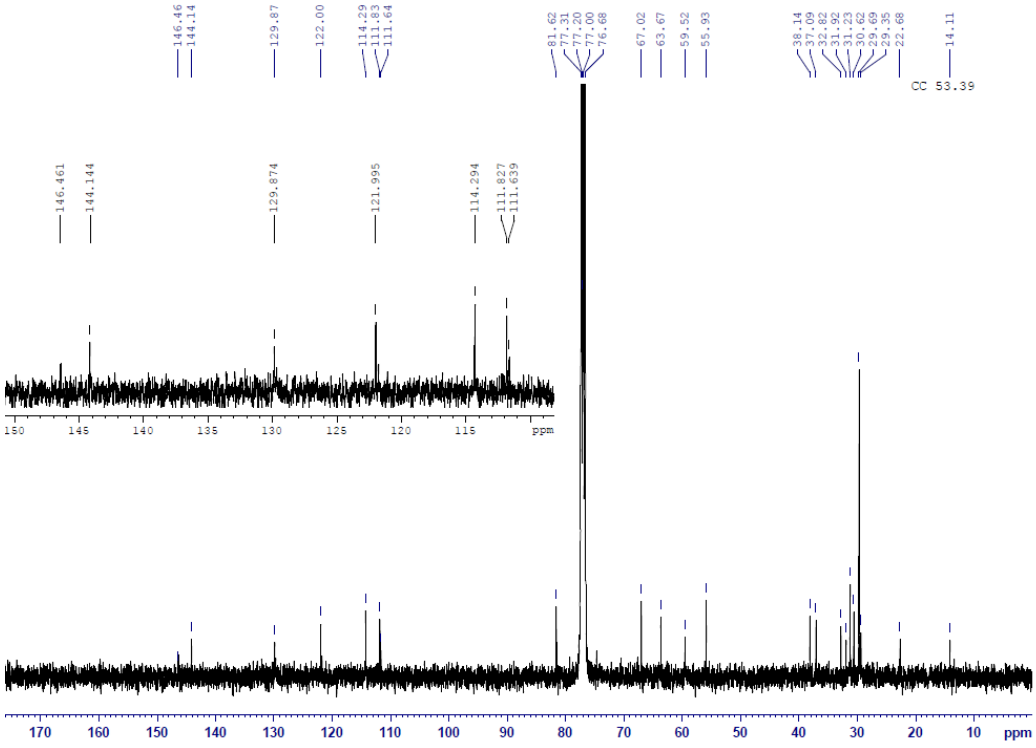
146.46
144.14
129.87
122.00
114.29
111.83
111.64
81.62
77.31
77.20
77.00
76.68
67.02
63.67
59.52
55.93
38.14
37.69
32.82
31.92
31.23
30.62
29.69
29.35
22.68
14.11
CC 53.39
ppm

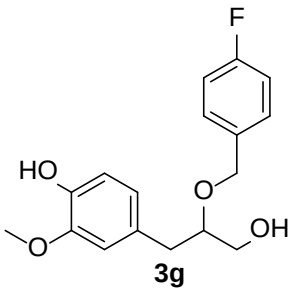
F
HO
O
OH
O

3g

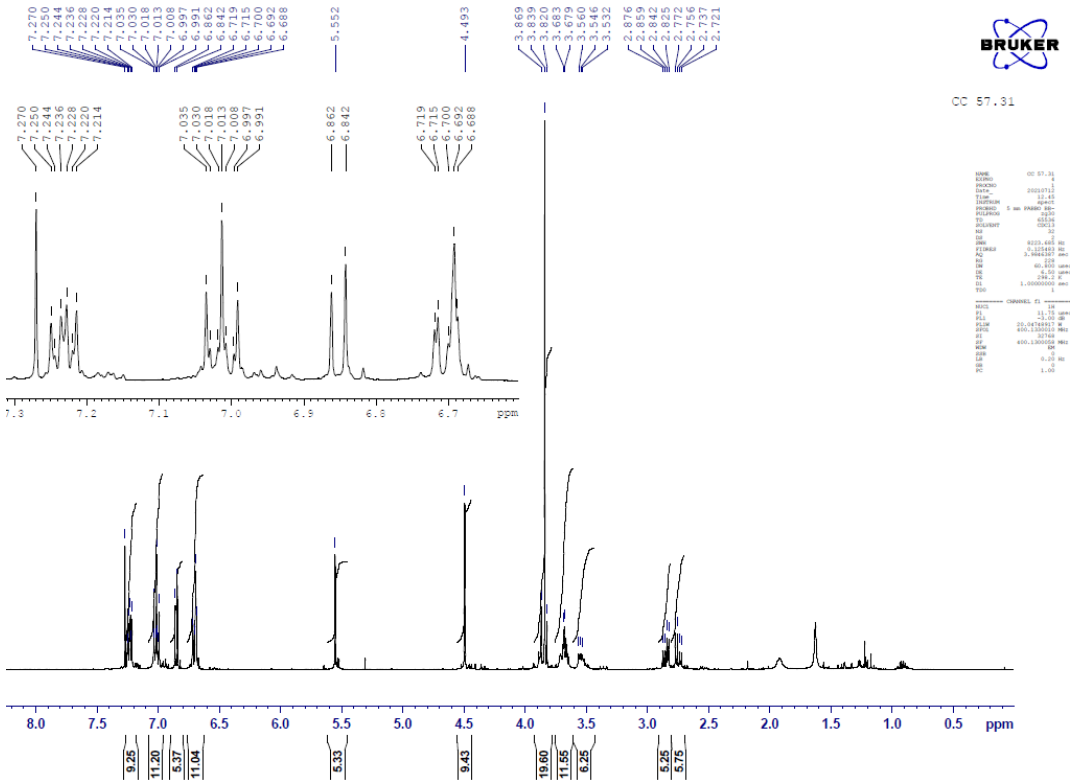
BRUKER
CC 57.31
8.0 7.5 7.0 6.5 6.0 5.5 5.0 4.5 4.0 3.5 3.0 2.5 2.0 1.5 1.0 0.5 ppm
9.25 11.20 5.37 11.04 5.33 9.43 19.60 11.55 6.25 5.25 5.75

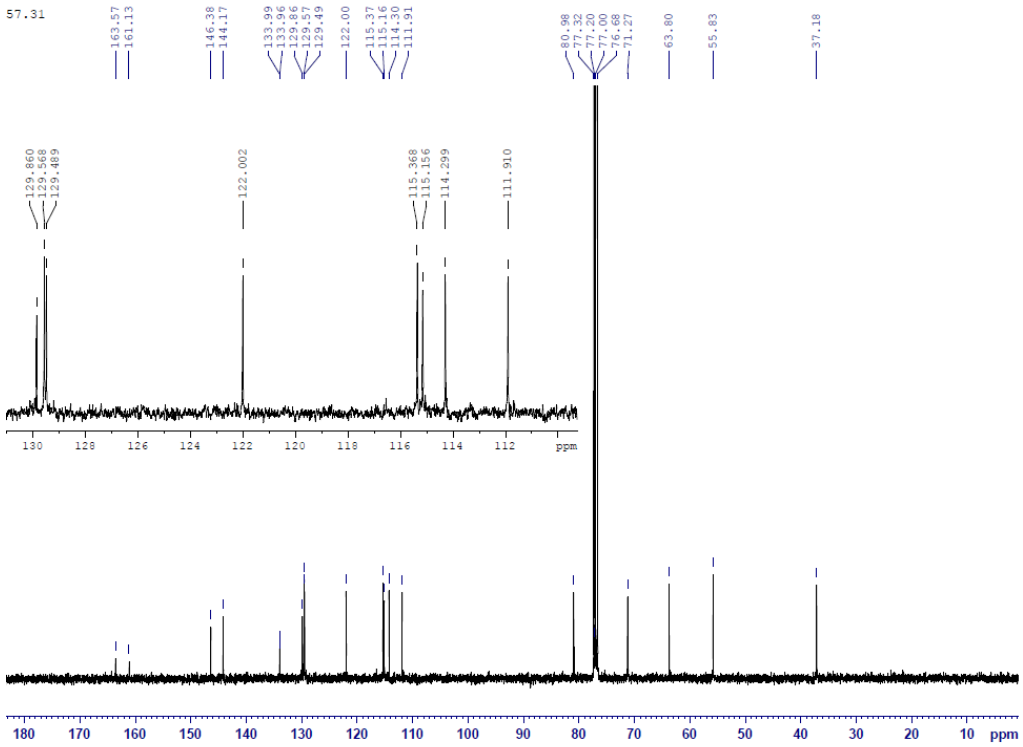
57.31
180 170 160 150 140 130 120 110 100 90 80 70 60 50 40 30 20 10 ppm